ELSEVIER

PII: S0032-3861(97)00298-X

Polymer Vol. 39 No. 2, pp. 291–298, 1998

0032-3861/97/$17.00+0.00

A direct comparison of spinodal decomposition analysis by time and *q* resolved light scattering and n.m.r.

N Parizel*, F Kempkes, C Cirman, C Picot and G Weill
Institut Charles Sadron, CNRS-ULP Strasbourg, 6 rue Boussingault, 67083 Strasbourg Cedex, France
(Received 23 October 1996; revised 17 January 1997)

Time and q resolved light scattering and nuclear magnetic resonance spin-lattice relaxation time have been performed on polystyrene/poly(vinyl methyl ether) blends during the early stage of the spinodal decomposition. The two techniques are used to determine the apparent diffusion coefficient at two different temperatures. A satisfying agreement is found between the results of T_1 n.m.r. measurements and those from light scattering. Otherwise, it has been shown that n.m.r. spin-lattice relaxation measurements, during the decomposition time, permits discrimination between spinodal decomposition and nucleation and growth. $T_{1\rho}$ experiments indicate that the homogeneous phase as well as the phase-separated quenched blend contain short scale inhomogeneities but it is not clear whether they compete with the larger scale spinodal decomposition process. © 1997 Elsevier Science Ltd.

(Keywords: polystyrene/poly(vinyl methyl ether) blends; spinodal decomposition; light scattering)

INTRODUCTION

While the effect of quasi spherical inclusions of one polymer A in another polymer B matrix on different mechanical properties, such as shock resistance or elastomer reinforcement has been extensively studied as a function of the inclusion size and the polymers' A and B viscoelestic properties, much less is known about bicontinuous dispersion of one polymer in the other. Such systems can be obtained from a solution of the precursor of the polymer A into a melt of polymer B upon polymerization of A[1]. It can also be achieved from spinodal decomposition in blends with lower critical solution temperature (LCST), where the extent of phase separation is controlled by the time following a temperature jump into the miscibility gap prior to the quench below the T_g of one of the separated phases. Shallow quenching between the critical temperature T_c and T_g before the deep quenching below T_g may be used to induce some redissolution and more finely tune the difference in composition of the separated phases[2]. Following the initial study of spinodal decomposition of the Polystyrene/Poly(vinyl methyl ether) blend by n.m.r., turbidity and microscopy, a number of more detailed studies using the time evolution of light, neutron or X ray scattering[3–7] as a function of wave vector, composition, and temperature above the spinodal have been performed. The n.m.r. method[8–14] on the other hand had not been pursued and a detailed comparison with the results of scattering methods is lacking. Since a comprehensive study of mechanical properties is difficult to carry out on the films required for scattering studies, n.m.r. characterization might be more convenient. These were the starting points for the investigation reported below.

* To whom correspondence should be addressed

MATERIALS AND METHODS

PVME ($M_n = 2.34\ 10^4$, $M_w/M_n = 2.28$) was purchased from Aldrich and carefully freeze dried from benzene. PS was synthesized by anionic polymerisation ($M_n = 1.32\ 10^5$, $M_w/M_n = 1.06$). The molecular weight distribution was obtained by GPC coupled with light scattering. The blends were evaporated from a 10% solution in toluene, dried first under static, then dynamic vacuum for three days. The resulting films (thickness $\approx 200\ \mu m$) were heated for two hours at 363 K to remove internal stresses and kept under vacuum to avoid exposure to moisture which, as shown by Hashimoto[15], may induce phase separation.

Light scattering experiments were carried out on a home built instrument, with a He-Ne laser source and a 38 photodiode array mounted on a mobile arm ($0 < \theta < 60°$) as detector. The films are mounted between glass covers and two thick metal blades, allowing low thermal inertia and temperature control within 0.5 K. The heating rate, temperature, position of the arm and data acquisition are controlled by a desk top computer. The software was developed in the laboratory.

^{1}H relaxation times in the laboratory (T_1) and in the rotating frame ($T_{1\rho}$) were measured on a Bruker SXP spectrometer operating at variable frequencies (30, 60, 90 Mhz). The resonance field is monitored with a field frequency lock (Drush n.m.r. gaussmeter and regulation unit TAO2) within 2 mT. T_1 measurements are carried by the inversion-recovery method. $T_{1\rho}$ was measured with a spin lock radio frequency field of amplitude $\gamma H_1 = 50$ kHz. The pulses are generated by a Hewlett Packard 8175 pattern generator ($90° = 5\ \mu s$) and the signals digitized using a 12 bits Le Croy 6810, at the fastest sampling rate of 5 Mhz, and finally averaged and treated on a desk top computer.

Glass transition temperatures of the homogeneous samples have been measured by scanning differential

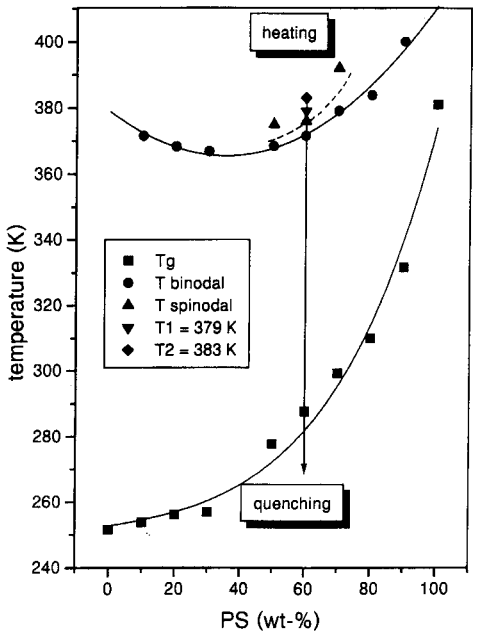

Figure 1 Phase diagram of the blend of PS/PVME and associated glass transition temperatures. Continuous lines are guides for the eyes

calorimetry (Perkin Elmer DSC 7) at a heating rate of 20 K min^{-1}. The composition dependence of T_g for a homogeneous blend is reported in *Figure 1*.

Cloud points are measured from the change in scattered intensity recorded at large q ($9.5\ 10^{-4}\ cm^{-1}$) with a slow heating rate (2 K min^{-1}). The corresponding binodal is reported on *Figure 1*.

Spinodal decomposition is triggered by a T jump from just below the binodal to a temperature above the spinodal and the scattered intensity recorded at variable q as a function of time t (see phase diagram). For n.m.r. measurements, films which have undergone the same heat treatment to the variable time t are rapidly quenched between two cold thick metallic plates.

Theoretical background

spinodal decomposition. Within the spinodal regime phase separation of a mixture of polymer is expected to proceed by continuous growth of the amplitude of composition fluctuations. The kinetics of the mechanisms of spinodal decomposition has been treated by Cahn[16] who showed that the maximum growth rate of the fluctuations occurs at a dominant mode wavelength. The Cahn kinetic theory is a generalization of the diffusion equation in inhomogeneous system. The starting point is the expression of the free energy of a binary mixture which is written in the imcompressible limit as:

$$F = \int [f(\phi) + \kappa(\nabla\phi)^2 + \cdots] \mathrm{d}v \qquad (1)$$

where $f(\phi)$ accounts for the free energy of the system having composition ϕ of one component (in the homogeneous system). The second term is the excess free energy resulting from the concentration gradient. By taking the variational derivative of equation (1) and applying the principle of continuity one is led to the diffusion equation:

$$\frac{\partial\phi}{\partial t} = D_c\left(\frac{\partial^2 f}{\partial\phi^2}\right)\nabla^2\phi - 2D_c\kappa\nabla^4\phi \qquad (2)$$

where D_c is the translational diffusion coefficient of molecules.

The solution of equation (2) is obtained as:

$$\phi(r) - \phi(0) = \Sigma\exp[R(q)t]\{A(q)\cos(q.r) + B(q)\sin(q.r)\}$$

with:

$$R(q) = D_c q^2\left\{-\left(\frac{\partial^2 f}{\partial\phi^2}\right) - 2\kappa q^2\right\} \qquad (3)$$

where $q = 2\pi/\lambda$ is the wavenumber of the spatial composition fluctuations and λ is the corresponding wavelength.

Since the scattered intensity is shown to be proportional to the square of the amplitude of the composition fluctuation $(\phi_1 - \phi_2)^2$, $R(q)$ is easily calculated from the time evolution of the scattered intensity:

$$I(q,t) = I(q,t=0)\exp[-2R(q)t] \qquad (4a)$$

De Gennes[17] proposed a theory of spinodal decomposition for incompressible, binary liquids composed of macromolecules in the context of the mean-field approximation. For a symmetrical blend of A and B polymers with the same degree of polymerization $N = N_A = N_B$ and identical Kuhn statistical segment lengths $a = a_A = a_B$ this author can derive the relaxation rate for the growth of fluctuations in the linear SD regime as:

$$R(q) = q^2\Lambda(q)\left\{2\chi - \frac{1}{N\phi(1-\phi)} - \frac{a^2q^2}{36\phi(\phi-1)}\right\} \qquad (5)$$

where $\Lambda(q)$ is the Onsager coefficient, which is given by:

$$\Lambda(q) = N\phi(1-\phi)D_c \qquad (6)$$

for the small q limit, i.e. for the case where SD is achieved by translational diffusion of polymer molecules A and B through the «reptation» process, D_c is the self-diffusion coefficient for translational diffusion of polymers, which is predicted to scale as N^{-2}. Thus from equation (5) and equation (6), it follows that

$$R(q) = q^2 D_c\left[\left(\frac{\chi-\chi_S}{\chi_S}\right) - \left(\frac{R_0^2}{36}\right)q^2\right] \qquad (7)$$

Consequently, in the general theory of Cahn

$$-\frac{\partial^2 f}{\partial\phi^2} = \frac{\chi-\chi_S}{\chi_S} \quad \text{and} \quad \kappa = R_0^2/72 \qquad (8)$$

The parameter χ_S is the χ parameter at spinodal temperature: $\chi_S = [2N\phi(1\text{-}\phi)]^{-1}$ and R_0^2 is the unperturbed chain dimension ($R_0^2 = Na^2$).

The linear theory can predict the wavenumber q_m of the spatial composition fluctuations that grow most rapidly in the SD regime and the maximum relaxation rate $R(q_m)$.

$$q_m^2 = q_c^2/2 = -(\partial^2 f/\partial\phi^2)/4\kappa \qquad (9)$$

$$R(q_m) = -D_c(\partial^2 f/\partial\phi^2)/8\kappa$$

In the SD regime, $(\delta^2 f/\delta\phi^2)$ is negative (the mixture being unstable for the infinitesimal fluctuations), and hence $R(q)$ can be positive for values of q smaller than the critical q (q_c).

So, plots of $R(q)/q^2$ vs q^2 based upon linear theory, allow several parameters to be determined.

$$D_{app} \equiv \frac{R(q)}{q^2}\Big|_{q=0} = D_c\left(\frac{\chi-\chi_S}{\chi_S}\right) \qquad (10)$$

$$q_m^2 = 1/2q_c^2 = \frac{18}{R_0^2}\left(\frac{\chi - \chi_S}{\chi_S}\right) \quad (11)$$

$$R(q_m)^{1/2} = \frac{3D_c^{1/2}}{R_0}\left(\frac{\chi - \chi_S}{\chi_S}\right) \quad (12)$$

In this context $R(q)$ should be proportional to q^2 and should depend on diffusivity D_c and thermodynamic driving force for the phase separation, $(\chi_S - \chi)/\chi_S$.

Strobl[18] pointed out that the Cahn-Hilliard treatment is incomplete, one shortcoming being the neglect of the random thermal forces responsible for the concentration fluctuations. The general equation, first given by Cook[19], also accounts for the experimental decrease of $I(q)$ with increasing q and validates relations (10)–(12) in our experimental conditions. The solution of the general equation of motion can be written as:

$$I(q,t) = I_\chi(q,0) + [I(q,t=0) - I_\chi(q,0)]\exp(-2R(q)t) \quad (4b)$$

with

$$I_\chi(q)^{-1} = \frac{1}{N\phi(1-\phi)} f_D^{-1}(\chi) - 2\chi$$

for symmetrical blends. $f_D(x)$ denotes the Debye structure factor of non-interacting ideal chains.

Relaxation and spin diffusion

Going from a homogeneous to a phase-separated system one expects the ^1H nuclear relaxation to evolve from one exponential to two exponentials with time constants and amplitudes determined by the composition and relative proton fractions of the two phases. In the case of T_1 or $T_{1\rho}$, this decomposition is only valid if the size of the microphases is larger than the root-mean-square path lengths over which spin diffusion takes place. In solids, spin diffusion occurs when two different spin temperatures[20,21] T_S exist within the sample. During spin-lattice relaxation measurements when two spin-lattice relaxation times are different enough in a sample, an equilibrium between the two spin temperatures is reached from hot spins to cold ones by spin diffusion. The nuclear spin magnetization can diffuse between the two regions in a time of the order of the longer relaxation time. Assuming three-dimensional diffusion, the RMS distance, $< 1^2 >^{1/2}$, is[22]

$$\langle 1^2 \rangle^{1/2} = (6D_S T_i)^{1/2} \quad (13)$$

where T_i is the relaxation time and D_S the spin diffusion coefficient[23–25]. If one considers that the spin-lattice relaxation time in the laboratory frame is of the order of one second and the spin-lattice relaxation time in the rotating frame of about ten milliseconds, the associated lengths are of order of 100 and 10 Å. Roughly, two spin systems possessing different T_1 values will seem to relax with only one T_1 if their populations are not further apart than 100 Å from each other. This is for example the case in polymers with CH_3 groups in the side chain at temperatures where the rotational jumps of the CH_3 group around the ternary axis is characterized by a correlation time $\tau_C \sim \omega_0^{-1}$ where ω_0 is the n.m.r. frequency. This makes the methyl protons acting as a sink for the whole nuclear magnetization. Assuming a number M_1 and M_2 of methyl and other protons, assuming the direct relaxation of M_2 protons to be infinitely long and a very fast spin diffusion between neighbouring 1 and 2 protons, i.e. a common spin temperature, one can write the relaxation of the total magnetization as[26]:

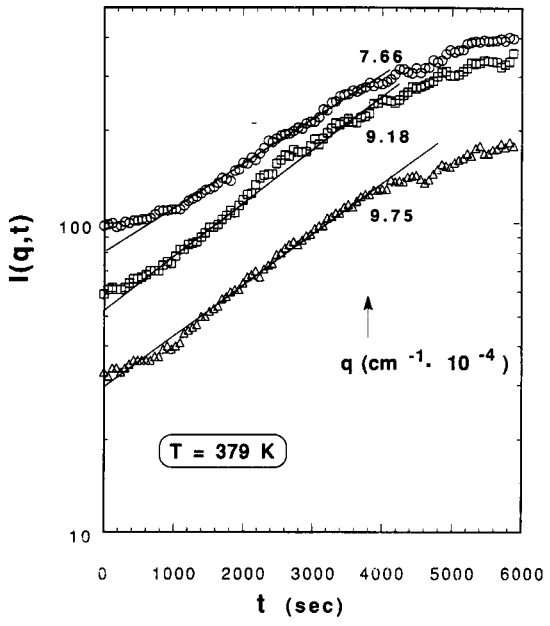

Figure 2 Time dependence of $I(q,t)$ at three q values after a T jump at 397 K. Lines are linear regressions of the initial part of the scattered signal. The points corresponding to the very early increase are not taken into account because they are affected by the temperature equilibrium of the sample. The accuracy corresponds to the size of the points

$$\frac{d(M_1 + M_2)}{dt} = -R_1 M_1 \quad (14)$$

leading to one exponential relaxation with a rate

$$R = R_1 \frac{M_1}{M_1 + M_2}$$

For biphasic systems with not infinitely fast spin diffusion and comparable relaxation rates, Douglass and McBrierty[27] have modelled the influence of spin diffusion using a simple coupling parameter to characterize the spin diffusion at the interface between the two phases where the spin temperature is assumed to be homogeneous.

The first order differential equation (15) and equation (16) describe the flow of energy associated with the magnetization M_i between phases and also to the lattice:

$$\frac{dM_1}{dt} = -R_1 M_1 - K_1 M_1 + K_2 M_2 \quad (15)$$

$$\frac{dM_2}{dt} = -R_2 M_2 - K_2 M_2 + K_1 M_1 \quad (16)$$

where M_1 and M_2 are the magnetization intensities associated with regions 1 and 2, respectively, $R_1 = 1/T_1(1)$, $R_2 = 1/T_1(2)$, and K_1 and K_2 are the parameters which control the strength of the diffusion coupling.

EXPERIMENTAL RESULTS

Light scattering

We concentrate on the 60 wt-% PS blend. The temperature of the binodal is found at 372 K (*Figure 1*). *Figure 2* displays the time dependence of the scattered intensity at three q values after a T jump at 379 K. At all times within the available q range $I(q)$ decreases when q increases, as

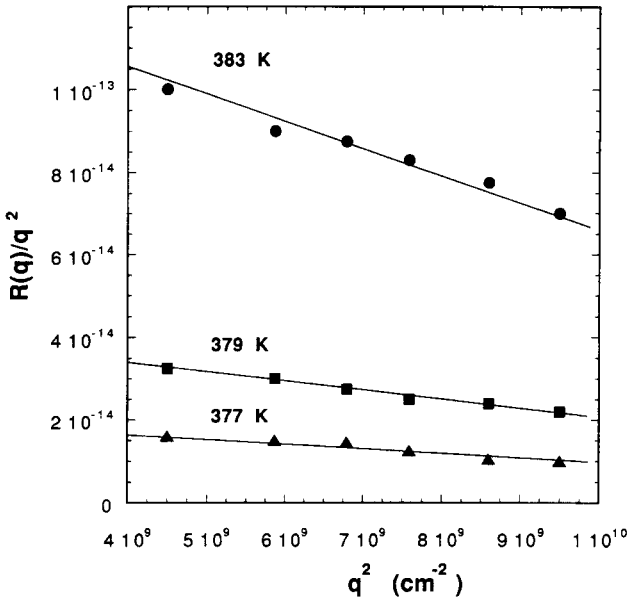

Figure 3 Variation of $[R(q)/q^2]$ as function of q^2. Lines are linear regressions. The accuracy of the measurements is around 8%

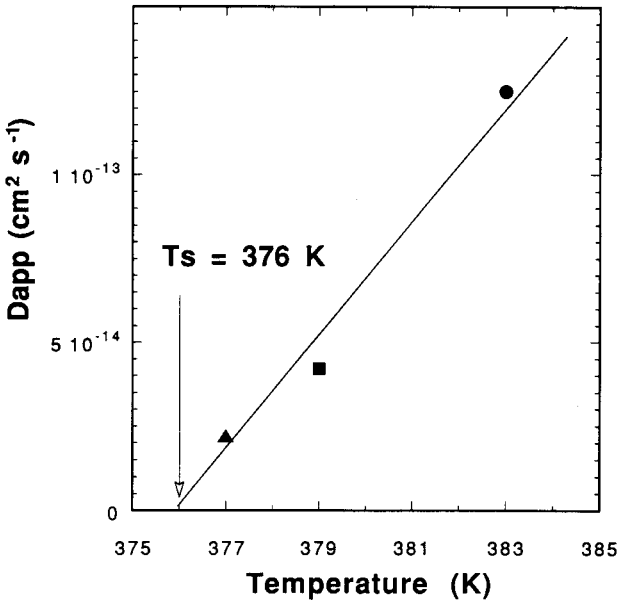

Figure 4 D_{app} dependence on the decomposition temperature. T_S is the spinodal temperature obtained by linear regression with an accuracy of ±0.2 K

Table 1 Apparent diffusion coefficient and most probable wavelength values for different temperatures (60wt-% PS blend)

T (°K)	D_{app}(cm^2/s)	λ_m(cm)
377	2.16 10^{-14}	6.8 10^{-5}
379	4.17 10^{-14}	6.0 10^{-5}
383	12.53 10^{-14}	6.0 10^{-5}

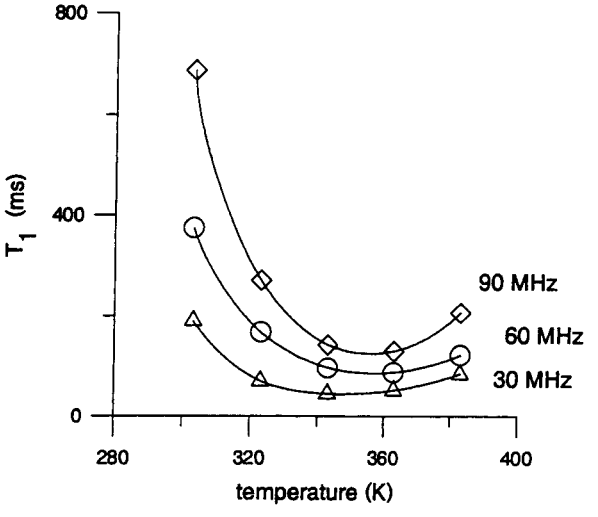

Figure 5 T_1 of the PVME vs magnetic field and vs temperature. The accuracy of measurements is around 10%

permitted by the general equation (4b), and we do not reach the maximum expected at $q_m = 2\pi/\lambda_m$. $R(q)$ increases however with q and from the plot of $R(q)/q^2$, (*Figure 3*), one can calculate, from the slopes and intercepts, using relations (10)–(12), the apparent diffusion coefficient D_{app} and the wavelength λ_m of the dominant fluctuation. The values at three temperatures are reported in *Table 1*. λ_m is nearly temperature independent, within experimental error $\lambda_m = 6400 \pm 400$ Å. This value, corresponding to $q_m = 10^5$ cm^{-1}, agrees with the absence of a maximum in the available q range ($q < 10^5$ cm^{-1}). Since however from the cloud point experiment, the composition of the PS rich phase in the phase diagram varies appreciably between the two extreme temperatures indicating a significant change of $\chi - \chi_S$, one would expect q_m to increase and λ_m to decrease. The insensitivity of λ_m with temperature may be due to the large polydispersity of PVME. On the other hand D_{app} increases with temperatures as it should since both D_c and $\chi - \chi_S$ increase with temperature. Extrapolation to $D_{app} = 0$ should provide the temperature of the spinodal. The variations of D_c and $\chi - \chi_S$ with temperature are not well defined, but a linear variation with temperature (*Figure 4*) leads to reasonable values. Similar experiments have been carried out for 50/50 and 70/30 blends and the corresponding temperature of the spinodal reported on the phase diagram in *Figure 1*.

N.M.R.

In order to choose the conditions where T_1 is the most sensitive to the composition of the phases, we have measured the T_1 of the homopolymers and homogeneous blends at 30, 60 and 90 Mhz at temperatures between 300 and 380 K. T_1 for PS is nearly constant, reflecting the absence of fast sub-glassy relaxations in this range of temperature. PVME T_1 has a strong minimum well above its glass transition temperature (*Figure 5*). In his original paper Nishi[13] has shown that in homogeneous blends the value of T_1 at the minimum is a sensitive linear function of the total protons to the number of protons in PVME, and that at the second sub-glassy minimum at 93 K in PVME a similar relation holds, resulting from spin diffusion to the mobile CH_3 group of PVME as explained above. Since we wanted to avoid systematic low temperature measurements but needed to work below T_g of the blends to avoid regression of the spinodal decomposition during n.m.r. measurements we have chosen to calibrate the values of T_1 close to the flat minimum at 60 Mhz and 303 K. Working at lower frequencies could enhance the contrast between the PS and PVME T_1 but at the expense of the signal to noise ratio

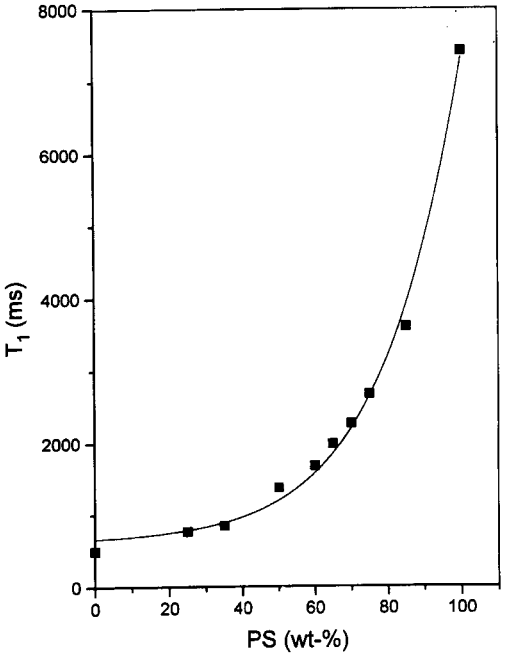

Figure 6 Calibrated curve T_1 (ms) vs PS wt-% for homogeneous blends. The accuracy of measurements is around 10%

Table 2 T_1 dependence of the 60/40 PS/PVME blend with decomposition time at 379 K

Decomposition time (s)	% Long T_1 % Short T_1	Long T_1 *(ms)* *Short* T_1 (ms)	PS wt-%of the PS rich phase
0	100	1678	60
300	92	1695	60.2
	8	472	57.7
600	93	1735	60.9
	7	462	48.0
1200	89	1788	61.8
	11	599	45.4
1800	85	1870	63.2
	15	540	41.9
		1973	64.9
3000	80	824	40.4
	20		
6000	78	2100	67.1
	22	710	34.8

Table 3 T_1 dependence of the 60/40 PS/PVME blend with decomposition time at 383 K

Decomposition time(s)	% Long T_1 % Short T_1	Long T_1(ms) Short T_1(ms)	PSwt-% of the PS rich phase
300	86	1856	62.9
	14	551	42.2
600	81	1920	64.0
	19	598	42.9
900	77	2026	65.8
	23	598	39.9
1800	73	2175	68.4
	27	592	38.4

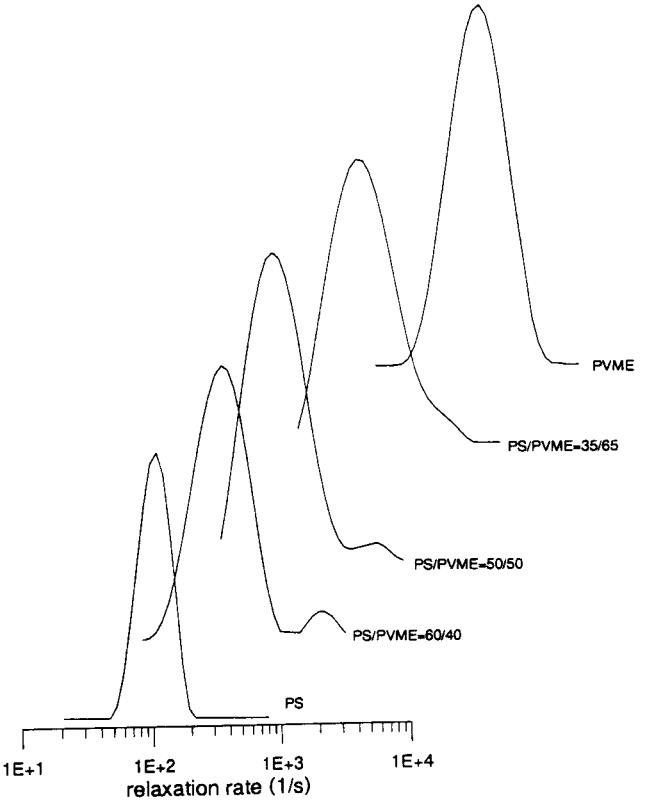

Figure 7 Inverse Laplace transforms of the $T_{1\rho}$ relaxation curve for the individual components and the homogeneous mixtures. (Note the logarithmic scale which makes the apparent area irrelevant in terms of the respective fractions of relaxing protons: see *Table 4*)

that we have to keep high enough to work on small homogeneously treated thin films. The calibration curve, built from the T_1 dependence of homogeneous blends with composition, under these conditions is given in *Figure 6*. Since the temperature of the minimum shifts with composition and we work on the low temperature rising side of the T_1 versus T curve, we do not expect a linear variation of T_1 with composition, but we can sensitively interpolate a composition from a value of T_1 corresponding to the range 50–80% PS.

Indeed, subjecting a 60% PS blend to an initial monoexponential spin lattice relaxation (T_1 = 1678 ms) a T jump of variable duration to 379 or 383 K followed by a fast quenching below the glass transition temperature, one observes a biexponential spin lattice relaxation. The decomposition parameters are given in *Table 2* and *Table 3*. The composition of the PS-poor phase has been calculated from the PS wt-% of the PS-rich phase and the conservation of mass.

Considering the size of the composition fluctuations as revealed by light scattering, one does not expect spin diffusion to play a significant role and one expects to obtain matching results from a study of T_1 or $T_{1\rho}$. Since $T_{1\rho}$ measured at 50 kHz and 300 K have been found respectively to be 8.20 ms for PS and 0.42 ms for PVME, a calibration curve has been sought for homogeneous blends. However relaxation in the rotating frame appears not to be precisely exponential for PS compositions higher than 25 wt-%, as shown in *Figure 7*, where the Laplace transforms of the relaxation have been performed using the CONTIN software[28,29]. This suggests that microheterogeneities may exist in the region of compatibility slightly above T_g which are large enough for spin diffusion to be insufficient at the time scale of $T_{1\rho}$. Therefore the calibration curve has been established using the $T_{1\rho}$ at the maximum of the two peaks of the relaxation spectrum. The associated values are reported in *Table 4* and *Figure 8*. Performing the $T_{1\rho}$ measurements for various decomposition times at 379 and 383 K and using the CONTIN software, three values of $T_{1\rho}$ are always found (*Figure 9*). The results of CONTIN analysis are given in *Table 5*

Table 4 Spin-lattice relaxation times in the rotating frame for the individual blend components and for the homogeneous blends

Sample	% Long $T_{1\rho}$ % Short $T_{1\rho}$	Long $T_{1\rho}$ (ms) Short $T_{1\rho}$ (ms)
PVME		0.42
PS 25wt-%		0.69
PS 35wt-%	53	1.60
	47	0.43
PS 50wt-%	62	3.08
	38	0.73
PS 60wt-%	64	4.12
	36	0.94
PS 65wt-%	78	4.93
	22	0.99
PS 70wt-%	79	5.99
	21	1.34
PS 75wt-%	85	6.38
	15	1.12
PS 85wt-%	92	6.84
	8	0.73
PS		8.20

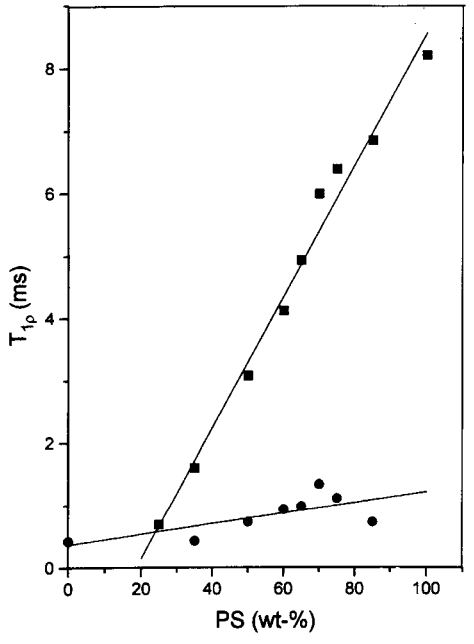

Figure 8 Calibrated curve of $T_{1\rho}$ (ms) vs PS wt-% for homogeneous blends. The accuracy of measurements is around 10%

Table 6. No significant difference is found between the two decomposition temperatures.

DISCUSSION

While the interpretation of light scattering is based on the existence of a predominant sinusoidal composition fluctuation, the n.m.r. results can only be interpreted in term of two homogeneous coexisting phases, that is, ignoring the nano scale heterogeneities as revealed from the $T_{1\rho}$ measurements. One can evaluate the coherence of the two interpretations from two points of view:

(i) does the phase composition obtained at long decomposition times match the phase composition obtained from the determination of the phase diagram (binodal).
(ii) does the time evolution of the composition and relative volume of the phases, as measured from T_1 results, match the time evolution of the scattered intensity.

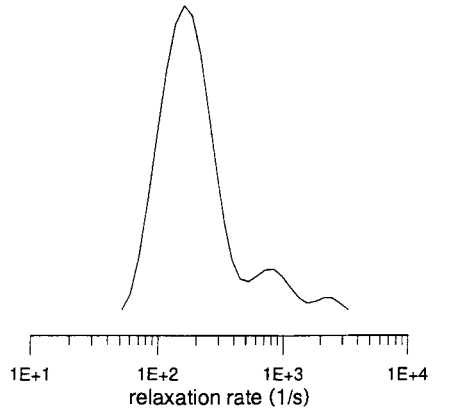

Figure 9 Inverse Laplace transforms of the $T_{1\rho}$ relaxation curve for a decomposed PS/PVME 60/40 blend in the SD regime

Table 5 $T_{1\rho}$ dependence of the 60/40 PS/PVME blend with the decomposition time at 379 K

Decomposition time (s)	% Long $T_{1\rho}$ % Intermediate $T_{1\rho}$ % Short $T_{1\rho}$	Long $T_{1\rho}$ Intermediate $T_{1\rho}$ Short $T_{1\rho}$
120	48	5.20
	34	1.68
	18	0.50
420	41	5.80
	33	1.80
	26	0.50
600	43	6.30
	37	1.95
	20	0.50
1200	43	6.50
	35	1.85
	22	0.50
1800	41	6.60
	34	2.10
	25	0.50
3000	45.5	6.30
	31.5	1.85
	23	0.50
6000	44.5	6.70
	30	2.00
	25.5	0.50

Table 6 $T_{1\rho}$ dependence of the 60/40 PS/PVME blend with the decomposition time at 383 K

Decomposition time (s)	% Long $T_{1\rho}$ % Intermediate $T_{1\rho}$ % Short $T_{1\rho}$	Long $T_{1\rho}$ Intermediate $T_{1\rho}$ Short $T_{1\rho}$
300	48	6.33
	25	1.88
	27	0.50
600	49	6.33
	25	1.70
	26	0.47
900	49	6.53
	24	1.64
	27	0.43
1800	48	6.69
	23	1.69
	29	0.43

From the T_1 calibrated curve, the accuracy is low in the region of short T_1, corresponding to the PVME rich phase, but high in the region of high T_1 corresponding to the PS rich phase. Indeed the values 67% and 68% given in *Tables 3 and 4* for 379 and 383 K are in good agreement with the

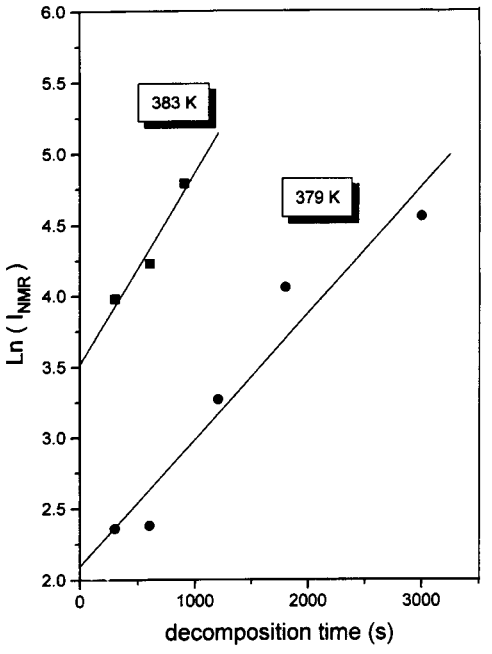

Figure 10 Ln ($I_{n.m.r.}$) vs the decomposition time. Lines are linear regressions according to relation 23. The confidence limits is around 14%

phase boundary on the PS rich side of the phase diagram, but the values 34.8 and 38.4 seem very high compared to the very flat phase boundary on the PVME rich side of the phase diagram.

To compare the values of D_{app} given by light scattering and by n.m.r. we remark that the scattered intensity of a phase separated binary mixture is given by[30]:

$$I(t) = \text{cste.}(\Delta n)^2[\phi_1(t) - \phi_2(t)]^2\varphi_1(t)\varphi_2(t) \qquad (17)$$

where Δn is the difference in refractive index of the two constituents, ϕ_1 and ϕ_2 the composition of the two phases, φ_1 and φ_2 their volume fractions. Ln ($I_{n.m.r.}$) has been recalculated from the values of ϕ_i and φ_i given in *Tables 3 and 4*. The result is given in *Figure 10*. The slopes s ($8.65\ 10^{-4}$ at 379 K and $1.3\ 10^{-3}$ at 383 K) should be compared to the values of $2R(q)$ for the dominant fluctuation, or to the value of D_{app} defined in relation (10).

$$s = 2D_{app}q_m^2 = \frac{8\Pi^2 D_{app}}{\lambda_m^2} \qquad (18)$$

Using the values of λ_m given in *Table 1* one gets $D_{app} = 4.5\ 10^{-14}\text{cm}^2\ \text{s}^{-1}$ at 379 K and $D_{app} = 5.9\ 10^{-14}\ \text{cm}^2\ \text{s}^{-1}$ at 383 K. In comparison with the values directly derived from light scattering (*Table 1*) there is good agreement at 379 K but the increase of D_{app} at 383 K is much smaller. This can be due to both the increasing uncertainties with decreasing slope in the extrapolations in *Figure 3* and to the fact that λ_m is nearly constant while it should decrease more rapidly with temperature.

Considering the experimental uncertainties of about 14% and the assumptions made in the interpretation of the data, the coherence of the n.m.r. and light scattering measurements is satisfactory.

One can ask if it is possible to assert only from the n.m.r. results that the phase separation observed is a spinodal decomposition. To confirm our previous interpretations, a nucleation and growth process is now envisaged. Besides the spinodal decomposition where the separation of the phases is due to composition fluctuations and where the size of the dominant fluctuation remains constant (λ_m) with the decomposition time, in a nucleation and growth process, the size of nuclei, here the PS-rich domains, increases and their composition is a constant with the decomposition time. Their composition is given by the phase boundary of the PS-rich side of the phase diagram or, if the n.m.r. technique is only considered, by the composition associated to the longest T_1 after a long enough decomposition time.

Initially, the measurement of the T_1 of the matrix, phase 1, of 60 wt-% PS gives the value of 1678 ms. Then, some nuclei, phase 2, appear with an intrinsic T_1 of 2175 ms at 383 K corresponding to a composition of 68 wt-% PS. The spin lattice relaxation curve of the mixture consists of two exponentials, their intensity x_i being proportional to the ^1H in each phase. During the growth of the nuclei, x_2 increases, x_1 decreases and T_{11} decreases because the matrix becomes poorer in PS. Consequently, the amplitude x_2 of the long T_1 (T_{12}) increases with decomposition time. Experimentally (*Tables 2 and 3*) the opposite tendency is observed. The only possibility to make x_2 decrease is that a transfer of magnetization via diffusion exists from the nuclei of PS-rich composition to the matrix and that this transfer increases with the decomposition time. Effectively a transfer from the PS-rich domains (T_1 = 2175 ms) to the matrix (T_1 < 1678 ms) can exist at the interface, the strength of the diffusion coupling being given by the parameters K_1 and K_2 in equations (15) and (16). In fact, the fit of the experimental relaxation curves with the solution of those equations leads to the increase of the parameter K with the decomposition time. Since, as the nuclei grow, there is less interface and less spin diffusion, it is impossible to reconcile increase spin diffusion coupling during the decomposition time with the growth of the nuclei. So, even considering an eventual contribution from spin diffusion, the n.m.r. results can't be reconciled with a nucleation and growth process.

Now compare the T_1 data with those of $T_{1\rho}$. T_1 for a homogeneous blend is monoexponential while it is often bi-exponential in the rotating frame. This indicates that nanoheterogeneities exist. Such heterogeneities have already been noticed in the literature: Schmidt-Rohr et al.[12] have studied a 50/50 weight percent blend of PS (200 000) and PVME (50 000). A nanoheterogeneous structure has been observed at 60 K above the glass transition temperature of the blend. Asano et al.[31] have shown from ^{13}C resolved ^1H T_1 and $T_{1\rho}$ measurements that while a unique $T_{1\rho}$ is observed for a 50/50 blend below T_g, three different $T_{1\rho}$ components are found at 311 K from the aromatic protons of PS, the methoxy and methine groups of PVME. This has been interpreted by the authors in term of a spatially homogeneous but motionally inhomogeneous blend. Khokhlov and Erukhimovich[32] have proposed that a non-local expression for the entropy of mixing may induce nanoheterogeneous structures in blends of polymers with widely different T_g values between the glass transition temperature and the binodal temperature of the blend.

The problem is therefore not the presence of these heterogeneities but to understand how this nanoheterogeneity interferes with the spinodal decomposition process on larger scales. A simple case would be that the nanoheterogeneity disappears at temperatures just below the binodal and plays no role in the spinodal decomposition. One would then assume that during the quenching, nanoheterogeneities reappear in the two homogeneous phases. One would then expect, in our case, to find for each phase a bimodal distribution of $T_{1\rho}$. Due to overlap, this is compatible with a trimodal distribution with the

longest value increasing regularly with time from a value of 4.12 ms towards a value of the order of 6 ms corresponding to the PS-rich phase and the shortest value decreasing correspondingly with time from a value of 0.9 ms to a value close to 0.4 ms. The extreme values are indeed observed at long times where the T_1 relaxation becomes independent of the decomposition time, typically 6000 s at 379 K and 1800 s at 383 K. But what is puzzling however is the fact that the $T_{1\rho}$ relaxation becomes independent of decomposition time at the very beginning of the decomposition where T_1 shows that the composition fluctuation is far from its maximum value, typically 1200 s at 379 K and 600 s at 383 K. Also there is some inaccuracy in the recording and CONTIN analysis of the $T_{1\rho}$ relaxation, not only the value of the long time seems very reliable, but the fraction of long, intermediate and short $T_{1\rho}$, is constant within experimental error. This puzzling result should be confirmed by more detailed studies using ^{13}C resolved ^{1}H T_1 and $T_{1\rho}$ measurements. These cannot however be carried out on thin film samples. We are therefore left again the problem of controlling spinodal decomposition in thick samples.

CONCLUSION

Comparison of the dynamic of spinodal decomposition as observed directly by light scattering or indirectly by ^{1}H T_1 relaxation on quenched samples indicates that n.m.r. alone can be used to follow and characterize the time evolution of the composition fluctuation to the final equilibrium binodal composition. This will permit the use of n.m.r. as the microscopic characterization technique for thick samples of bi-continuous blends on which detailed mechanical experiments can be performed. The characterization of the nanoheterogeneities observed in ^{1}H $T_{1\rho}$ data between the glass transition and the binodal temperature could simultaneously be performed by ^{13}C resolved ^{1}H $T_{1\rho}$ measurements. Further experiments will benefit from the use of a blend with a less polydisperse PVME component resulting in a less flat and more symmetrical phase diagram.

REFERENCES

1. Paul, D. R. and Newman, S., *Polymers Blends*. Academic Press, New York, 1978.
2. Kammer, H. W., *J. Macromol. Sci. Chem.*, 1990, **A27**(13/14), 1713.
3. Scripov, V. P. and Scripov, A. V., *Sov. Phys. Ups.*, 1979, **22**, 389.
4. Snyder, H. L., Meakin, P. and Reich, S., *Macromolecules*, 1983, **16**, 757.
5. Bates, F. S. and Wilzius, P., *J. Chem. Phys.*, 1980, **72**, 4756.
6. Nishi, T. and Kwei, T. K., *Polymer*, 1975, **16**, 285.
7. Hashimoto, T., Kumaki, J. and Kawai, H., *Macromolecules*, 1983, **16**, 641.
8. Caravatti, P., Neuenschwander, P. and Ernst, R. R., *Macromolecules, 1985*, **18**, 119.
9. Caravatti, P., Newenschwander, P. and Ernst, R. R., *Macromolecules, 1986*, **19**, 1889.
10. Mirau, P. A. and Bovey, F., *Macromolecules*, 1990, **23**, 4548.
11. Mirau, P. A., White, J. L. and Heffner, S. A., *Macromol. Symp.*, 1994, **86**, 181.
12. Schmidt-Rohr, K., Clauss, J. and Spiess, H. W., *Macromolecules*, 1992, **25**, 3273.
13. Kwei, T. K., Nishi, T. and Roberts, R. F., *Macromolecules*, 1974, **7**, 667.
14. Nishi, T., Wang, T. T. and Kwei, T. K., *Macromolecules*, 1975, **8**, 227.
15. Hashimoto, T., Itakura, M. and Shimidzu, N., *J. Chem. Phys.*, 1986, **85**, 6773.
16. Cahn, J. W., *Trans. Metal. Soc. AIME*, 1967, **242**, 166.
17. de Gennes, P. G., *J. Chem. Phys.*, 1980, **72**, 4756.
18. Strobl, G. R., *Macromolecules*, 1985, **18**, 558.
19. Cook, H. E., *Acta Metall.*, 1970, **18**, 297.
20. Abragam, A., in *The Principles of Nuclear Magnetism*. Oxford University Press, Oxford, 1961.
21. Abragam, A., and Goldman, M., in *Nuclear Magnetism: Order and Disorder*. Oxford University Press, New York, 1982.
22. Bloembergen, N., *Physica*, 1949, **15**, 386.
23. Cheung, T. T. P., *Phys. Rev.*, 1981, **B23**, 1404.
24. Cheung, T. T. P. and Gerstein, B. C., *J. Appl. Phys.*, 1981, **52**, 5517.
25. Li, K. L., Jones, A. A., Inglefield, P. T. and English, A. D., *Macromolecules*, 1989, **22**, 4198.
26. McBrierty, V. J., and Packer, K. J., in *Nuclear Magnetic Resonance in Solid Polymers*. Cambridge University Press, 1993, p. 77.
27. Douglas, D. C. and McBrierty, V. J., *J. Chem. Phys.*, 1971, **54**, 4085.
28. Provencher, S. W., *Comput. Phys. Commun.*, 1982, **27**, 213.
29. Provencher, S. W., *Comput. Phys. Commun.*, 1982, **27**, 229.
30. Kerker, M., in *The Scattering of Light*. Academic Press, New York and London, 1969.
31. Asano, A., Takegoshi, K. and Hikichi, K., *Polymer*, 1994, **35**, 5630.
32. Khokhlov, A. R. and Erukhimovich, I. Y., *Macromolecules*, 1993, **26**, 7195.